Vibrational spectroscopy of acid treated vermiculites

Michal Ritz[a*], Jana Zdrálková[b,c], Marta Valášková[b,c]

[a] Regional Material and Technology Centre, VŠB-Technical University of Ostrava, 17. listopadu 15, 708 33 Ostrava-Poruba, Czech Republic

[b] Nanotechnology Centre, VŠB- Technical University Ostrava of Ostrava, 17. listopadu 15, 708 33 Ostrava-Poruba, Czech

[c] IT4Innovations Centre of Excellence, VŠB-Technical University of Ostrava, 17. listopadu 15/2172, CZ-708 33 Ostrava-Poruba, Czech Republic

*Corresponding author

tel.: +420 597 323 370; fax.: +420 597 321 675;

E-mail address: michal.ritz@vsb.cz

Abstract

The natural vermiculites from different localities (Bulgaria, Brazil, and South Africa) after acid treatment were used for this study. Differently acidified vermiculite samples were prepared from the natural vermiculite sample using different concentrations of hydrochloric acid (0.5 M and 1 M) and different reaction time (2 h and 4 h) at 80°C. Natural vermiculites and acid treated vermiculites were analyzed by elemental analysis, X-ray diffraction (XRD) analysis and studied using Fourier transform infrared (FTIR) spectroscopy and dispersive Raman spectroscopy. According to the XRD analysis vermiculites are interstratified

DSpace VŠB-TUO http://hdl.handle.net/10084/101847 26/5/2014

structures created in the different two-one-zero sheet hydrated phases. Ratio of intensities of spectrally deconvoluted bands at 1075 cm^{-1} and 1000 cm^{-1} (stretching vibration of Si-O bonds of vermiculites and stretching vibration of Si-O bonds of amorphous silica, respectively) was used to determine of the content of amorphous silica in acid treated vermiculite samples. Study of the infrared and Raman spectra of the acidified vermiculites enable a comparison of these two spectroscopic data that have not yet been performed.

Keywords

Vermiculite, acid treatment, elemental analysis, XRD analysis, IR spectroscopy, Raman spectroscopy

1. Introduction

Vermiculites are secondary 2:1 clay minerals (phyllosilicates) formed primarily by alteration of mica and less commonly by alteration of amphibole, chlorite, olivine, pyroxene or other clay minerals. The 2:1 layer is composed of one octahedral sheet between two tetrahedral sheets. The positive charge deficiency is compensated by the hydrated exchangeable cations Mg^{2+}, Ca^{2+}, Na^{2+} and K^{+} located in the interlayer space between the parallel 2:1 layers. Macroscopic vermiculite occurs in four types of host rocks: (1) ultramafic and mafic; (2) gneiss and schist; (3) carbonate rocks; and (4) granitic rocks, and each of these has characteristic features. The major commercial deposits belong to the first category. Structural analysis revealed predominantly mixed-layer vermiculite-biotite or vermiculite-phlogopite composition [1].

Vermiculites show the diversity of properties related to the structural characteristics, such as layer charge associated with the numerous isomorphic substitutions, mixed layered

DSpace VŠB-TUO http://hdl.handle.net/10084/101847 26/5/2014

structure and to dehydration-rehydration ability. The existence of a number of definite states of hydration and the regular interstratification of layers with a basal spacing of 2.060 nm were determined as consistence of approximately regular alternations of 1.150 nm and 0.902 nm layered domains [2]. The variation of basal reflections corresponding to the interstratified one-zero sheet hydrate (*d*-values of 1.04 nm) with probably a random interstratified phase of two- and one-sheet hydrates (*d*-values of 1.28 nm) in vermiculite from Llano (Texas, USA) were studied using powder neutron diffraction [3]. Reflection with *d*-value 1.002 nm was detected in a phlogopitic vermiculite from Madagascar [4]. Those authors highlighted the existence of two superstructures formed by a regular 1:1 interstratification with *d*(001) = 2.541 nm (the result of alternation of layers with basal spacings of 1.376 nm and 1.165 nm) and with *d*(001) = 2.153 nm (the result of alternation of layers with basal spacings of 1.151 nm and 1.002 nm).

Acid activated clay minerals find wide industrial applications as catalysts or catalyst supports [5-7]. Several workers studied structure of smectites after treatment with the hydrochloric acid [7-11] and sulphuric acid [6, 12, 13]. A comparable study of the swellable clay minerals was conducted after leaching by H_2SO_4 and HCl of different concentrations [14]. Authors have found that acidified smectites had higher specific surface area than the original materials and displayed still the ability to exchange cations.

Selective acid leaching is an important method for preparing porous materials. The leached vermiculite shows a microporous structure with good thermal and hydrothermal stability and acidic properties. The residual porous silica has a higher specific surface area in comparison with original vermiculite. The effect of grinding was studied on the formation of porous materials by acid-leached vermiculite [15]. Authors observed the most significant difference in the values of specific surface area between ungrounded (504 m^2 g^{-1}) and grounded (720 m^2 g^{-1}) vermiculite leached with 1 M HCl. The catalytic properties of leached

DSpace VŠB-TUO http://hdl.handle.net/10084/101847 26/5/2014

vermiculite were characterized as pre-cracking matrices of heavy oil fractions [16]. Many authors have primary used FTIR spectroscopy to follow the changes of the acid treated smectites and vermiculites. In comparison with IR spectroscopy, one of the advantages of Raman spectroscopy lies in the fact that Raman spectra do not contain overtone and combination band [17]. Additionally, Raman spectroscopy allows simple arrangement of solids samples without the preparation of pellet. The most handicap of Raman spectroscopy is occurrence of fluorescence. Since the Raman effect is very weak even relatively small fluorescence can overlap Raman bands. The probability of exciting fluorescence falls off substantially at long wavelength of laser [18].

So far, in the literature there are not many studies on the IR and Raman spectroscopy of the vermiculites and acidified vermiculites and their comparison are lacking. The aim of this study was to assess changes in the IR and Raman spectra of three natural vermiculites from different localities after their treatment with the 0.5 M and 1 M hydrochloric acid for 2 and 4 h.

2. Samples and methods

2.1 Samples

Three natural vermiculites of different mineralogical origin, supplied by Grena, Co., Czech Republic, were chosen as the natural material for the present study. Vermiculite from northwestern region of Bulgaria (designated as V1) is found in calc-alkaline rocks, biotite-hornblende granodiorites and tonalities [19] that apparently resulted from the action of rain water on the biotite (phlogopite). Vermiculite from the Santa Luzia mine in the Paraiba region of Brazil (designated as V2) resulted from the change of phlogopite and biotite and occurs mainly within zones of complex mafic, ultramafic and carbonatite. Vermiculite from Palabora mine in the Limpopo province of South Africa (designated as V3) is product of hydration of

DSpace VŠB-TUO http://hdl.handle.net/10084/101847 26/5/2014

phlogopite/biotite occurring in the phlogopite and apatite rich pyroxenites. The vermiculite from Palabora was described as mixed-layer vermiculite-phlogopite with the content less than 50% vermiculite [20].

2.2 Acid treatment

All samples were milled in a vibratory mill for 3 minutes. The particle size fractions less than 0.004 mm were obtained by sieving and then were used for acid treatments. An amount of 5 g of powdered native vermiculite samples were placed in the reagent flasks and treated with 200 ml of acid solutions. Two different concentrations of 0.5 mol/dm^{-3} (0.5 M) and 1 mol/dm^{-3} (1 M) aqueous solution of hydrochloric acid were used. Designation of acid treated samples is in the Table 1.

The acid leaching was performed in glass vessel at temperature 80°C for 2 and/or 4 h. The obtained suspensions were washed several times with demineralized water to remove chlorides (it was checked by silver nitrate test). Then samples were centrifuged (frequency of rotation was 4000 rpm; centrifugation time was 7 minutes.) and dried at 80°C overnight.

2.3 Infrared spectroscopy

IR spectra of vermiculite samples were measured by potassium bromide pellets technique. Exactly 2.0 mg of sample was ground with 200 mg dried potassium bromide. This mixture was used to prepare the potassium bromide pellets. The pellets were pressed by 8 tons for 30 seconds under vacuum. The IR spectra were collected using FT-IR spectrometer Nexus 470 (ThermoScientific, USA) with DTGS detector. The measurement parameters were the following: spectral region 4000-400 cm^{-1}, spectral resolution 4 cm^{-1}; 64 scans; Happ-Genzel apodization. Treatment of spectra: polynomial (second order) baseline, subtraction spectrum

DSpace VŠB-TUO http://hdl.handle.net/10084/101847 26/5/2014

of pure potassium bromide. IR spectra of all samples of vermiculite (natural and after exposure to acid) were measured under above mentioned conditions.

2.4 Raman spectroscopy

A 180° degree sampling was used as measurement technique. Only vermiculite samples (without additional substances) were used for measurement of Raman spectra at dispersive Raman spectrometer DXR SmartRaman (ThermoScientific, USA) with CCD detector. The measurement parameters were as follows: excitation laser 780 nm, grating 400 lines/mm, aperture 50 μm, exposure time 1 second, number of exposures 500, spectral region 2500-50 cm^{-1}. An empty sample compartment was used for background measurement. Treatment of spectra: fluorescence correction (6^{th} order).

2.5 Elemental analysis

The elemental analysis of Si, Al, Ca and Ti was performed using the energy dispersive X-ray fluorescence spectrometer Spectro Xepos (Spectro Analytical Instruments, Germany). Sample were mixed with the wax and pressed into the pellets.

The elemental analysis of Na, K, Mg, and Fe was determined also using an atomic emission spectrometer with inductively coupled plasma Spectro Vision (Spectro Analytical Instruments, Germany) after total sample decomposition in hydrochloric and hydrofluoric acids and acid mixture (H_3PO_4 + H_2SO_4 + H_3BO_3) [21]. The content of Fe^{2+} was determined using titration with 0.1 M solution of $K_2Cr_2O_7$ after the previous decomposition of each sample in hydrochloric and hydrofluoric acids in a carbon dioxide atmosphere, according to Czech norm CSN 722041 Part 11.

2.6 X-ray powder diffraction analysis

DSpace VŠB-TUO http://hdl.handle.net/10084/101847 26/5/2014

The X-ray powder diffraction (XRD) patterns were measured on the X-ray diffractometer Ultima IV RIGAKU (reflection mode, Brag-Brentano arrangement, $CuK\alpha_1$ radiation) in ambient atmosphere under constant conditions (40 kV, 40 mA). The CuKα2 was removed by the Rachinger method which is based on separation of overlapping α1 and α2 components in PDXL: Integrated X-ray powder diffraction software.

3. Results and Discussion

3.1 Elemental analysis

Content of elements in vermiculite samples expressed in oxides form is in Table 2. The structural formulas of original vermiculites V1, V2, and V3 were calculated per half unit cell composition based on the results from the elemental analysis as follows:

V1 $(Si_{3.12}Al_{0.88})\,(Al_{0.01}Fe^{3+}_{0.36}Fe^{2+}_{0.05}Mg_{2.56}Ti_{0.02})\,O_{10}\,(OH)_2\,Mg_{0.06}\,Ca_{0.11}Na_{0.02}K_{0.05}$

V2 $(Si_{3.12}Al_{0.88})\,(Al_{0.05}Fe^{3+}_{0.37}Fe^{2+}_{0.03}Mg_{2.50}Ti_{0.05})\,O_{10}\,(OH)_2\,Ca_{0.10}Na_{0.05}K_{0.17}$

V3 $(Si_{3.10}Al_{0.78}\,Fe^{3+}_{0.12})\,(Fe^{3+}_{0.25}Fe^{2+}_{0.08}Mg_{2.51}Ti_{0.06})\,O_{10}\,(OH)_2\,Ca_{0.19}Na_{0.02}K_{0.33}$

Differences among the compositions of the three studied vermiculite minerals are evident. Especially, the variable K_2O content in the samples V1, V2, and V3 (0.8, 1.8, and 4.8 wt.%, respectively) suggest that studied samples are not pure vermiculites (Table 2). The small content of Mg^{2+}cation in the interlayer is in the V1 and none Mg^{2+}cation in the interlayer of V2 and V3. Vermiculite V3 contains tetrahedral Fe^{3+} which is characteristic of biotite (ferriphlogopite), as evidenced by earlier studies [22].

The octahedral composition of the vermiculites V1, V2, and V3 previewed in the ternary diagram (not presented here) compiled by [23] on the basis of the octahedral composition of vermiculites and hydrobiotites to trioctahedral micas suggests that those vermiculite samples are derived from trioctahedral micas of phlogopite type.

From the Table 2 it is obvious that the decrease of elemental content was caused by dissolution of the elements during the acid treatment. The biggest decrease (in absolute

DSpace VŠB-TUO http://hdl.handle.net/10084/101847 26/5/2014

amount) is evident for aluminum and magnesium. The decrease of elemental content was caused by dissolution of the elements during the acid treatment. Increase of elemental content can be traced only for silicon. However, an increase of silicon content was only relative (because of decrease of content of other elements). Similar behavior of elements during acid treatment of clay minerals were described in number studies e.g. [24].

3.2 X-ray powder diffraction analysis

The XRD pattern of V1 (Fig. 1a) shows the most intense characteristic (002) basal reflection of vermiculite with the interlayer space *d* (002) = 1.430 nm and basal reflections in further sequence. An additional low-intense reflection of wide profiles with the interlayer space value *d* = 1.24 nm and 0.8 nm were assigned to the random interstratified phase of two- and one layers of water. Significantly different layered structure of vermiculites V2 and V3 can be seen on their diffraction patterns in Figs. 1b and 1c. The XRD pattern of V2 (Fig. 1b) proved the interstratified layered structure with the prevailing presence of transitional phases between two layers of water in the interlayer space (*d*(002)=1.410 nm) and a lower content of water molecules (*d*(001)=1.240 nm). The superstructure with *d*(001) = 2.235 nm is the result of alternation of layers with the basal spacings of 1.410 nm and 0.833 nm [25,26]. The XRD pattern of V3 (Fig. 1c) proves the results of earlier study, that this mixed-layer vermiculite-phlogopite contains less than 50% vermiculite [20]. The vermiculite basal reflection (002) corresponding to the interlayer space (*d*(002)=1.442 nm) with the presence of two layers of water is less intense than reflections belonging to the interstratified layers with one-water layer (*d*(001)=1.206 nm). Weakly intense reflection with the value *d*(001) = 1.02 nm corresponds to the zero-water layers in the interstratified structure. The superstructure containing domains composed of mixtures of layers with one layer of water molecules in the interlayer space in a mixture with the two- or zero- water layers shows the reflection with

DSpace VŠB-TUO http://hdl.handle.net/10084/101847 26/5/2014

d(001) = 2.650 nm. The XRD patterns show different interstratification from prevailing vermiculite layers over layers of phlogopite in V1 and V2 to the prevailing phlogopite layers over vermiculite layers in V3.

After acid treatment of V1, V2 and V3 the basal reflection (*d*(002)=1.4 nm) on the XRD patterns of V1C, V2C and V3 is missing and only reflection with *d*(001)=1.2 nm, corresponding to the interstratified structure with lower content of water molecules, and also the superstructure (*d*(001) =2.6 nm, *d*(003) = 0.8 nm, and *d*(006) = 0.46 nm) are maintained. The XRD pattern of the sample V3C (Fig. 1c) is evidence of mica-like phase in a interstratified structure, as can be deduced by basal reflections *d*(001) =1.02 nm, *d*(002) = 0.493 nm, and *d*(003) = 0.350 nm.

3.3 Infrared spectroscopy

Spectra of all natural vermiculites are shown in Fig. 2. The pictured spectra seem to be relatively similar but they are different in a few weak bands. The assignment of the most vibration bands was performed according [10, 27, 28].

The broad band at 3400 cm^{-1} is attributed to stretching vibrations of O-H bonds of water. Small shoulders at 3710 cm^{-1} and 3670 cm^{-1} can be assigned to the stretching vibration of vermiculite structural O-H bonds. Band at 3670 cm^{-1} is present in all three spectra; band at 3710 cm^{-1} is present only in spectra of samples V2 and V3. According [29] both this bands are related to vibration of OH bond associated to interlayer cations. The presence of band at 3710 cm^{-1} in spectra of V2 and V3 confirm a structural difference in interlayer water between vermiculite V1 and others two vermiculites (V2 and V3); see subsection 3.2. The last band related to vibration of OH bond is spectral band at 1650 cm^{-1} (deformation vibration of O-H bonds of water); this band is presented in all three spectra of natural vermiculites.

DSpace VŠB-TUO http://hdl.handle.net/10084/101847 26/5/2014

Intensive band at 1000 cm^{-1} is due to stretching vibration of Si-O bonds of vermiculites. In the all three spectra are also seen band at 1075 cm^{-1} (as shoulder in intensive bands at 1000 cm^{-1}); this band can be assigned to stretching vibration of Si-O bonds of amorphous silica. Other bands which can be assigned to stretching Si-O vibration of amorphous silica are seen at 955 cm^{-1} and 815 cm^{-1}. Band at 955 cm^{-1} is present as small shoulder only in spectrum of V3; band at 815 cm^{-1} is seen as weak band in all three vermiculite spectra. The weak bands at 730 cm^{-1}, 670 cm^{-1} and 520 cm^{-1} are related to in plane deformation vibration of Al-O-Si bonds of vermiculites; band at 520 cm^{-1} is seen as shoulder in intensive band at 450 cm^{-1}. And finally, intensive band at 450 cm^{-1} can be assignment to deformation vibration of Si-O-Si bonds of vermiculites.

The spectral changes between natural and acid treated vermiculites were very similar for vermiculites from all three localities. In Fig. 3, the spectra are performed for the vermiculite from Brasil (samples V2, V2A-V2C). The most significant spectral changes are seen in the region 1300 cm^{-1} - 800 cm^{-1}. In this region, the natural vermiculites showed the most intensive band at 1000 cm^{-1} whereas the acid treated vermiculites at 1075 cm^{-1}. The band at 1000 cm^{-1} is due to the stretching vibration of Si-O bonds (as state above); this band is typical for vermiculites and for other phyllosilicates, too. The band at 1075 cm^{-1}, belonging to the stretching vibration of Si-O bonds of amorphous silica, points to the formation of amorphous silica in the acid treated clay minerals. This spectral (and also phase) changes of the clay minerals during acid treatment have previously been described e.g. [28]. Formation of amorphous silica due to acid treatment of vermiculites could be confirmed from the spectral changes also by increasing of shoulder at 955 cm^{-1} and weak band at 815 cm^{-1}.

Other spectral changes were more subtle. One of these changes could be seen by decreasing of deformation spectral bands of bond Al-O-Si (730 cm^{-1}, 670 cm^{-1} and 520 cm^{-1}). Decrease of these three bands is related to decrease of content of aluminum in the acid treated

DSpace VŠB-TUO http://hdl.handle.net/10084/101847 26/5/2014

vermiculites (see Tab. 2). Another subtle spectral change was the disappearance of bands of stretching vibration of structural OH groups (at 3710 cm^{-1} and 3670 cm^{-1}). These bands were seen only in the spectra of natural vermiculites, not in the spectra of acid treated vermiculites.

According to [10], formation of amorphous silica and its spectral manifestations are depending on the structure of used clay minerals. The authors found that behavior of dioctahedral and trioctahedral smectites was quite different. The formation of amorphous silica was faster for the trioctahedral smectites and the significant band of amorphous silica was observed already after 3 h acid treatment with 0.25 M HCl. For the dioctahedral smectites, the significant band of amorphous silica was evident even after 12 h exposure in 6 M HCl. The spectral changes in our studied vermiculites are very similar to those observed in trioctahedral smectites [10] and therefore we can assume their trioctahedral structure. This premise was confirmed by results of XRD analysis (see subsection 3.2).

3.4 Bands deconvolution analysis

The above discussed spectral bands in the region 1300 cm^{-1} - 800 cm^{-1} were relatively large overlapped. A spectral deconvolution of spectral bands of all measured vermiculite spectra by PeakResolve software (an integral part of spectroscopic software Omnic, ThermoScientific, USA) was performed for their comparison. The aim of band deconvolution analysis was to obtain information about numbers and wavenumbers of bands presented in important and (unfortunately) overlapped part of spectra. Another objective of this analysis was to determine the exact value of absorbance of overlapped bands; these were mainly important for band of stretching vibration of Si-O bonds in phyllosilicates (at 1000 cm^{-1}) and band of the stretching vibration of Si-O bonds of amorphous silica (at 1075 cm^{-1}). These two bands are too close to each other and there is not possible (without band deconvolution analysis) to determine exact value of absorbance these two bands.

DSpace VŠB-TUO http://hdl.handle.net/10084/101847 26/5/2014

The spectra of all vermiculite samples after spectral deconvolution contained three bands: 1075 cm^{-1}, 1000 cm^{-1}, and 955 cm^{-1}. Moreover the spectrally separated spectra of all acid treated vermiculites contained band at 1200 cm^{-1}. The separated spectra of vermiculites from Brazil and South Africa (natural and acid treated) showed spectral band with maximum at 925 cm^{-1}.The assignment of spectral bands at 1075 cm^{-1}, 1000 cm^{-1}, and 955 cm^{-1} is described above. Spectral band at 1200 cm^{-1} was reported in literature e.g. [10, 14] but without assignment. Due to the fact the band was presented only in spectra of acid treated vermiculites it could be assumed that this band belongs to vibration of amorphous silica. Spectral band at 925 cm^{-1} is attributed to deformation vibration of Al-Al-OH bonds (see [10]).

The ratio of intensity (RI) of spectral bands at 1075 cm^{-1} and 1000 cm^{-1} ($RI = I_{1075} / I_{1000}$) was calculated for all separated spectra of vermiculite samples. This ratio indicates an increase of amorphous silica bands (1075 cm^{-1}) in relation to the band of Si-O tetrahedral vibration (1000 cm^{-1}), as we can see in Fig. 4.

From the graph it is evident that RI of above mentioned bands was dependent on the acid concentration and reaction time. The highest increase of RI of amorphous silica band occurred during acid treatment of vermiculite from Bulgaria, while after acid treatment of vermiculite from Brazil increase of intensity of amorphous silica band was less significant. Vermiculite from South Africa showed the smallest changes in the RI of discussed bands. This observation corresponded to assumption, that sample from Palabora (V3) contains less than 50% of vermiculite (see chapter 2.1).

3.5 Raman spectroscopy

Whereas measurement of IR spectra of vermiculite is relatively routine, measurement of vermiculite Raman spectra is rather more complicated. The fluorescence was very intensive and mostly superimposed whole Raman spectra of vermiculites (as well as of other clay

DSpace VŠB-TUO http://hdl.handle.net/10084/101847 26/5/2014

minerals). Therefore it is necessary to find such measurement procedure which could minimize the fluorescence as well. One of the possibilities is the application of the excitation laser from the region of higher wavelengths. In our study, we used a laser 780 nm.

The structural changes among vermiculites from different localities detected by XRD analysis are much more evident in the Raman spectra than in IR spectra. The reason is very probably the fact that the Raman spectra (opposed to IR spectra) were measured in the region of lattice vibration (400 cm^{-1} – 50 cm^{-1}). Assignment of Raman bands of vermiculite is described in the literature very rarely. In addition, Raman bands of vermiculite are assigned unambiguously. In the study, assignment of Raman bands of vermiculite was performed according to [30].

Raman spectra of natural vermiculite V1 and also its acid treated samples V1A-V1C are different from others spectra of vermiculite samples. The spectra of samples V1 and V1C are shown in Fig. 5. The spectrum of sample V1 show weak bands at 100 cm^{-1} and 155 cm^{-1} that can be assigned to vibration of interlayer cations. Weak band at 190 cm^{-1} is attributed to the deformation vibration of Mg-O-Mg bonds. Medium intense band at 235 cm^{-1} is related to deformation vibration of O-Si-O bonds and medium band at 310 cm^{-1} can be assigned to deformation vibration of Si-O-Si bonds. Strong band at 410 cm^{-1} is attributed to the deformation vibration of O-Mg-O bonds. The weak band at 460 cm^{-1} is related to deformation vibration of O-Si-O bonds and medium intense band at 520 cm^{-1} are attributed to the deformation vibration of O-Mg-O bonds. Strong band at 630 cm^{-1} and shoulder at 670 cm^{-1} may arise from the stretching vibration of Mg-O bonds while medium band at 750 cm^{-1} is related to the stretching vibration of Si-O bonds. The described bands are almost negligible in the spectra of sample V1C. Moreover the band of vibration of interlayer cations (located at 100 cm^{-1} in spectrum of sample V1) is shifted at 90 cm^{-1} and second band of this vibration (located at 155 cm^{-1} in spectrum of sample V1) is not visible in spectrum of sample V1C. The

DSpace VŠB-TUO http://hdl.handle.net/10084/101847 26/5/2014

changes in the ratio of spectral bands can be observed in the spectrum of V1C (in comparison with the sample of natural vermiculite). The largest change is seen in bands at 630 cm^{-1} and 670 cm^{-1}. The band at 670 cm^{-1} is only small shoulder of band at 630 cm^{-1} in spectrum of V1, whereas the intensity of both bands are almost the same in the spectrum of V1C. The minor change in the ration of bands is in the bands at 310 cm^{-1} a 235 cm^{-1}. The both bands are the same intensive in the spectrum V1; the band at 235 cm^{-1} is more intensive then the band at 310 cm^{-1} in the spectrum of V1C. The alteration in structure of vermiculite V1 after acid treatment can be deduced from changes of ratio of these spectral bands.

As stated above, Raman spectra of vermiculite from others two localities (V2 and V3) were different from vermiculite V1. The spectra of vermiculite V2 and V3 showed the same spectral bands and spectral behavior of their acid treated samples was very similar. However, spectrum of V3 and also spectra of acid treated vermiculites (V3A-V3C) was affected by strong fluorescence and only weak bands and relatively high level of noise was observed. Example of Raman spectra of samples V2 and V2C is shown in Fig. 6. The bands of vibration of interlayer cations are seen at 100 cm^{-1} and at 120 cm^{-1}. Band of deformation vibration of Mg-O-Mg at 185 cm^{-1} is relatively highly intensive (opposed to spectrum of sample V1). Bands of deformation vibration of silicon bonded to oxygen are seen at 220 cm^{-1} (O-Si-O bonds) and at 290 cm^{-1} (Si-O-Si bonds).The bands of deformation vibration of O-Mg-O are visible at 350 cm^{-1} and at 530 cm^{-1} and they are relatively weak. Band at 290 cm^{-1} and also band at 350 cm^{-1} were absent in spectra of V1. Finally, weak band at 550 cm^{-1} and strong band at 670 cm^{-1} are due to stretching vibration of Mg-O bonds. In almost all bands we can observe decrease of intensity in spectra of acid treated samples V2C, except the bands at 220 cm^{-1} and at 290 cm^{-1}. Intensity of band at 290 cm^{-1} increased in spectra of acid treated vermiculite V2C while intensity of band at 220 cm^{-1} remains almost the same. The spectral band of interlayer cations vibration at 120 cm^{-1} si not present in the spectra of V2C.

DSpace VŠB-TUO http://hdl.handle.net/10084/101847 26/5/2014

From these spectral manifestation is seen that structural changes of acid treated vermiculite from Bulgaria are slightly different from those in acid treated vermiculites from other both localities. Spectral changes in band of vibration Si-O and Mg-O are present in spectra vermiculite from Bulgaria while only spectral change in band of vibration Si-O is seen in spectra others vermiculites.

4. Conclusions

The paper presents new findings on the structure of vermiculites based on the combined methods study. The XRD analysis revealed that natural vermiculites have interstratified layered structure with zero-, one- and two-layers of water molecules between layers, which correspond to the various stages of transformation from biotite (phlogopite, chlorite) to vermiculite. Acidified vermiculites compared with the original vermiculites exhibited loss of layers to each other regularly loaded in the layered structure, as evidenced by decrease of intensities of basal reflections. In addition, further loss of interlayer water molecules, as well cations are assumed by smaller interlayer distances.

The differences between structures of V1, V2 and V2 arising from the XRD analysis were also seen in their IR spectra that confirms differences in interlayers and in sample V3 also small content of vermiculite . Unlike XRD analysis, the infrared spectroscopy revealed amorphous silica in the acid treated vermiculites.

Band deconvolution analysis was used for characterisation of overlapped bands in the region from 1300 cm^{-1} to 800 cm^{-1} for all vermiculite samples. Intensity ratio of the spectral bands at 1075 cm^{-1} and 1000 cm^{-1} (I_{1075} / I_{1000}) after spectral separation calculated for acid treated vermiculites increased according to the acid concentration and reaction time.

Found differences between Raman spectra of sample V1 and samples V2 and V3 point out different structure of studied vermiculites (see subsections 3.1 and 3.2). Structural

DSpace VŠB-TUO http://hdl.handle.net/10084/101847 26/5/2014

differences were observed only in spectra of acid treated vermiculites. Contrary to infrared spectra, Raman spectra do not allow discerns the difference among the Si-O bond vibration of vermiculite and amorphous silica.

Vibrational spectroscopy confirmed the appropriate supportive and complementary technique to XRD analysis. Studies of the Raman spectra of vermiculites have not been so often presented in comparison with the IR spectra. This work confirmed that the results obtained from Raman spectroscopy has been a useful addition to the reliable identification of the structures of vermiculites.

Acknowledgments

This work was supported by the Czech Science Foundation (project No. P210/11/2215).

This paper was also created by the project No. CZ.1.05/2.1.00/01.0040 "Regional Materials Science and Technology Centre" within the framework of the operation program "Research and Development for Innovations" financed by the Structural Funds and from the state budget of the Czech Republic and IT4Innovations Centre of Excellence (project reg. No. cz.1.05/1.1.00/02.0070).

DSpace VŠB-TUO http://hdl.handle.net/10084/101847 26/5/2014

References

[1] W.A. Bassett, Amer. Min. 44 (1959) 282-299.

[2] G.F. Walker, Clay Clay Min. 4(1956) 101-115.

[3] D.R. Collins, A.N Fitch, R.A. Catlow, J. Mat. Chem. 8 (1992) 865 –873.

[4] H.G. Reichenbach, J. Beyer, Clay Min. 29 (1994) 327 –340.

[5] C.N. Rhodes, D.R. Brown, J. Chem. Soc. Faraday Trans. 88 (1992) 2269-2274.

[6] P. Komandel, M. Janek, J. Madejová, A. Weeks, C. Breen, J. Chem. Soc. Faraday Trans. 93 (1997) 4207-4210.

[7] J. Ravichandran, J. Sivasankar, Clays Clay Miner. 45 (1997) 854-858.

[8] I. Novák, B. Číčel, Clays Clay Miner. 26 (1978) 341-344.

[9] P. Komandel, D. Schmidt, J. Madejová, B. Číčel, Appl. Clay Sci. 5 (1990) 13-122.

[10] J.Madejová, J. Bujdák, M. Janek, P. Komandel, Spectrochim. Acta A 54 (1998) 1397-1406.

[11] H. Pálková, J. Madejová, D. Righi, Clays Clay Miner. 51 (2003), 133-142.

[12] C. Breen, J. Madejová, P. Komandel, J. Mater. Chem. 5 (1995) 469–474.

[13] M. Önal, Y. Sarikaya, Powder Technol. 172 (2007) 14-18.

[14] A. Stuedel, L.F. Batenburg, H.R. Fischer, P.G. Weidler, K. Emmerich, Appl. Clay Sci. 44 (2009) 105-115.

[15] C. Maqueda, A.S. Romero, E. Morillo, J.L. Pérez-Rodríguez, Phys. Chem. Solids 68 (2007) 1220-1224.

[16] H. Suquet, S. Chevalier, C, Marcilly, D. Barthomeuf, Clay Miner. 26 (1991) 49-60.

[17] R.L. Frost, P.M. Fredericks, Spectrochim. Acta A 49 (1993) 667-674.

[18] N. Sheppard, in: J.M. Chalmers, P.R. Griffits (Eds.) Handbook of Vibrational Spectroscopy, Vol. 1, John Wiley and Sons, Chichester, 2002, pp. 1-32.

[19] A. Seghedi, Turkish J. Earth Sci. 21 (2012) 669-721.

DSpace VŠB-TUO http://hdl.handle.net/10084/101847 26/5/2014

[20] H.F. Muiambo, W.W. Focke, M. Atanasova, I. van der Westhuizen, L.R. Tiedt, Appl. Clay Sci. 50(2010) 51-57.

[21] J. Seidlerová, H. Otoupalíková, M. Nováčková, Chem. Listy101 (2007) 165-170 (in Czech)

[22] H. Annersten, S. Devanarayanan, L. Häggström, R. Wäppling, Physica Status Solidi (a) 48 (1971) K137–K138.

[23] M.D. Föster, Clay Clay Min. 10 (1963) 70 –89.

[24] C. Maqueda, J.L. Pérez-Rodríguez, J. Šubrt, N. Murafa, Appl. Clay Sci. 44 (2009) 178-184.

[25] C. Marcos, A. Argüelles, A. Ruíz-Conde, P.J.Sánchez-Soto, J.A. Blanco, Mineral. Mag. 67(2003) 1253-1268.

[26] M. Valášková, J. Tokarský. K. Čech Barabaszová, V. Matějka, M. Hundáková, E. Pazdziora, D. Kimmer, Appl. Clay Sci. 72 (2013) 110–116.

[27] J. Madejová, Vib. Spectrosc. 31 (2003) 1-10.

[28] P. Komandel, J. Madejová, in: F. Bergaya, B.K.G. Theng, G. Lagaly (Eds.) Handbook of Clay Science, Elsevier, 2006, 263-287

[29] L. Chmielarz, M. Wojciechowska, M. Rutkowska, A. Adamski, A. Wegrzym, A. Kowalczyk, B. Dudek, P. Boron, M. Michalik, A. Matusiewicz, Catalysis today 191(2012) 25-31.

[30] M. Arab, D. Bougeard, K.S. Smirnov, Phys. Chem. Chem. Phys. 4 (2002) 1957-1963.

DSpace VŠB-TUO http://hdl.handle.net/10084/101847 26/5/2014

Figures captions

Fig. 1: XRD diffraction patterns of natural and acid treated vermiculites

Fig. 2: IR spectra of natural vermiculites

Fig. 3: IR spectra of natural and acid treated vermiculites in spectra region 1300-800 cm^{-1}

Fig. 4: Ratio of intensities of spectral bands at 1075 cm^{-1} and 1000 cm^{-1}

Fig. 5: Raman spectra of natural and acid treated vermiculites (V1 and V1C)

Fig. 6: Raman spectra of natural and acid treated vermiculites (V2 and V2C)

DSpace VŠB-TUO http://hdl.handle.net/10084/101847 26/5/2014

Table 1
List of analyzed vermiculite samples

Sample	Description of samples
V1	raw vermiculite from Bulgaria
V1A	sample V1 treated with 0.5 M HCl for 4 h
V1B	sample V1 treated with 1 M HCl for 2 h
V1C	sample V1 treated with 1 M HCl for 4 h
V2	raw vermiculite from Brazil
V2A	sample V2 treated with 0.5 M HCl for 4 h
V2B	sample V2 treated with 1 M HCl for 2 h
V2C	sample V2 treated with 1 M HCl for 4 h
V3	raw vermiculite from South Africa
V3A	sample V3 treated with 0.5 M HCl for 4 h
V3B	sample V3 treated with 1 M HCl for 2 h
V3C	sample V3 treated with 1 M HCl for 4 h

DSpace VŠB-TUO http://hdl.handle.net/10084/101847 26/5/2014

Table 2
Content of elements in raw and acid treated vermiculite samples

	w/w %								
Sample	SiO_2	TiO_2	Al_2O_3	Fe_2O_3	FeO	CaO	MgO	Na_2O	K_2O
V1	37.1	0.7	10.0	6.2	0.8	1.5	23.2	0.2	0.8
V1A	53.7	0.8	6.6	4.6	1.1	1.2	14.8	0.1	0.5
V1B	55.2	0.6	5.9	3.9	1.3	1.2	13.7	0.1	0.5
V1C	60.6	0.6	4.7	4.2	1.2	1.3	11.8	0.1	0.4
V2	36.7	0.9	10.8	6.5	0.5	1.8	20.0	0.4	1.8
V2A	56.8	1.0	6.9	5.4	0.3	1.4	10.8	0.2	1.8
V2B	58.9	0.4	6.3	4.9	0.4	1.5	9.9	0.2	1.8
V2C	59.2	0.8	6.2	4.8	0.5	1.5	9.8	0.2	1.8
V3	32.9	1.0	8.7	6.7	1.3	4.3	20.2	0.2	4.8
V3A	50.8	1.3	7.3	6.4	0.8	1.3	15.5	0.1	3.8
V3B	49.7	1.2	7.5	6.6	0.8	1.3	15.9	0.1	4.0
V3C	54.0	1.1	6.6	5.8	0.8	1.3	14.3	0.1	3.5

DSpace VŠB-TUO http://hdl.handle.net/10084/101847 26/5/2014

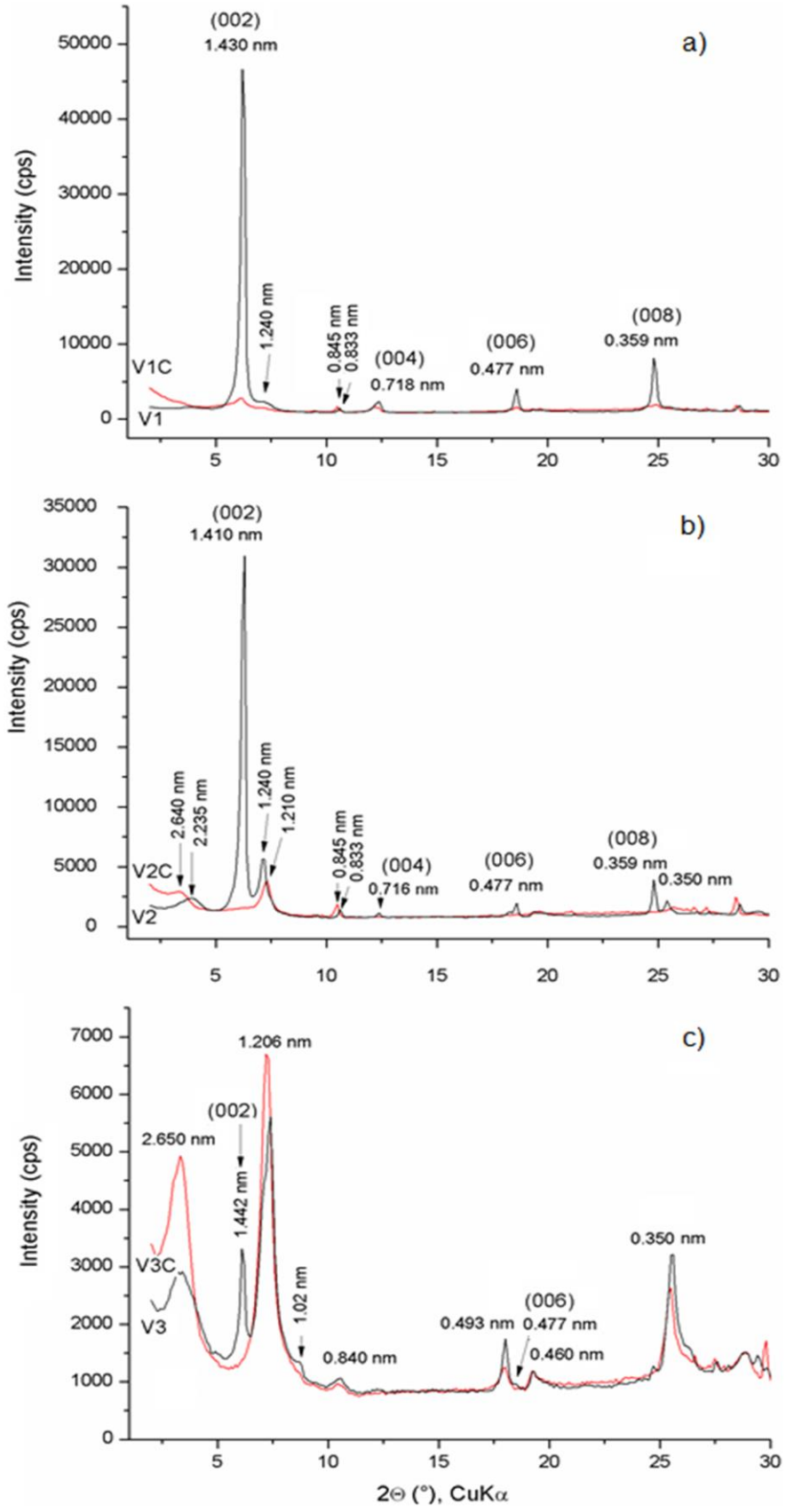

Fig. 1: XRD diffraction patterns of natural and acid treated vermiculites

DSpace VŠB-TUO http://hdl.handle.net/10084/101847 26/5/2014

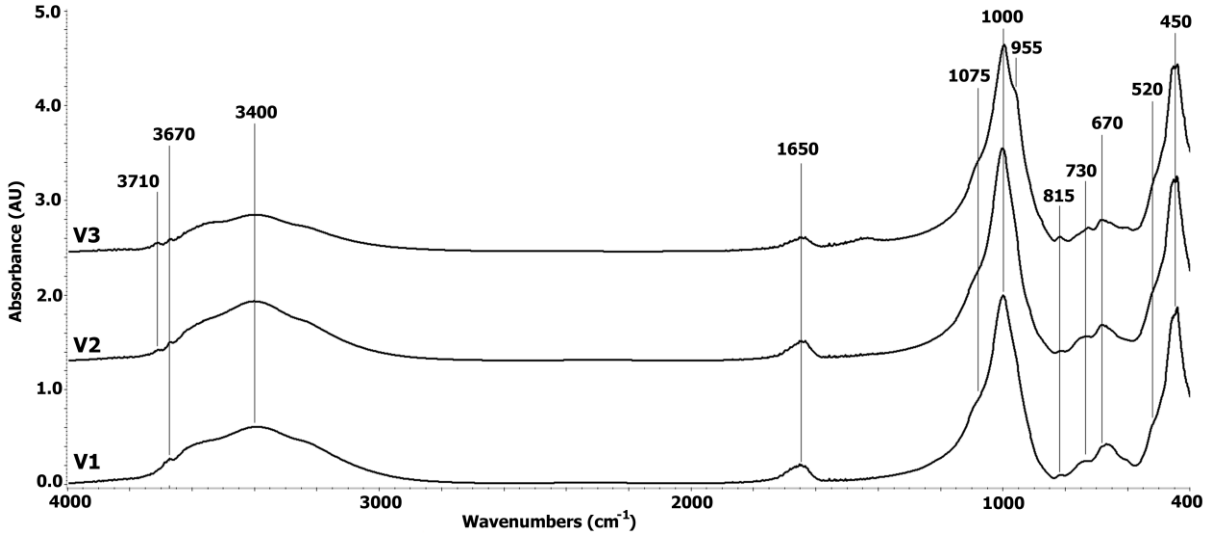

Fig. 2: IR spectra of natural vermiculites

DSpace VŠB-TUO http://hdl.handle.net/10084/101847 26/5/2014

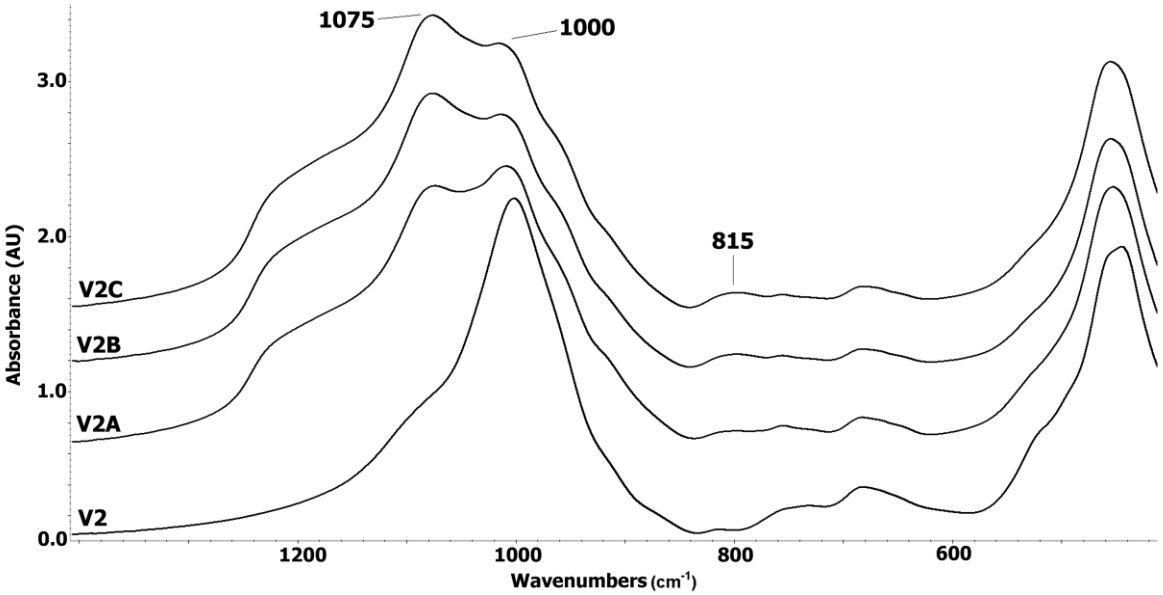

Fig. 3: IR spectra of natural and acid treated vermiculites in spectra region 1300-800 cm^{-1}

DSpace VŠB-TUO http://hdl.handle.net/10084/101847 26/5/2014

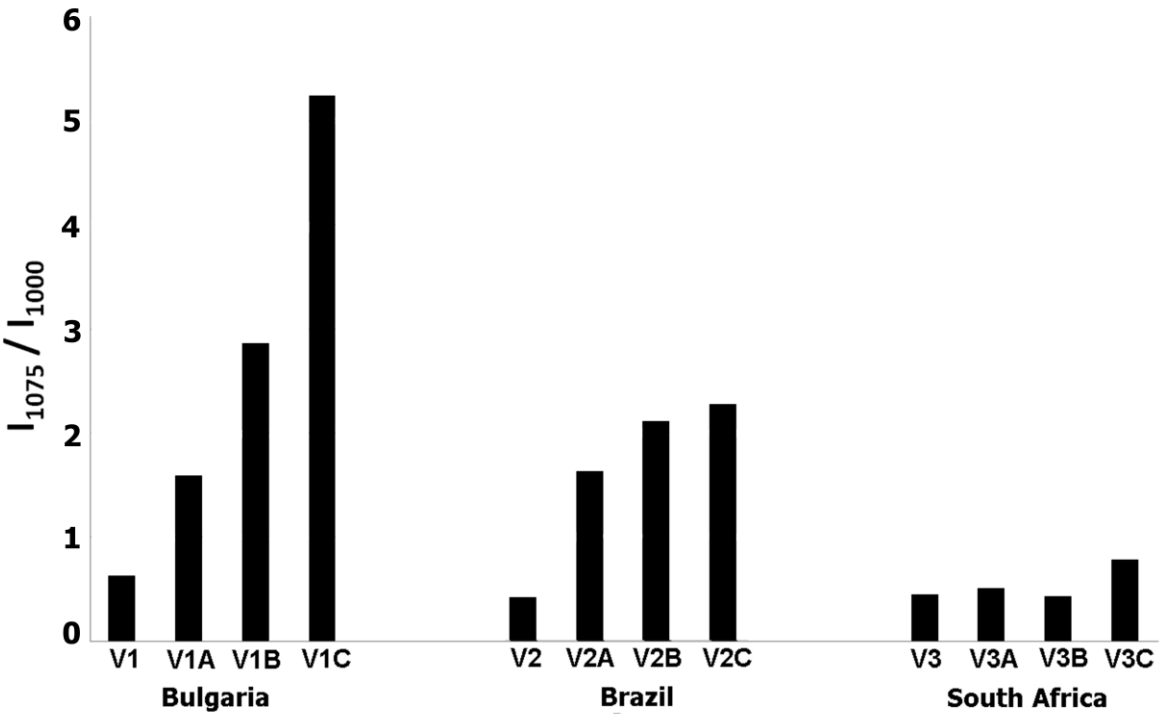

Fig. 4: Ratio of intensities of spectral bands at 1075 cm^{-1} and 1000 cm^{-1}

DSpace VŠB-TUO http://hdl.handle.net/10084/101847 26/5/2014

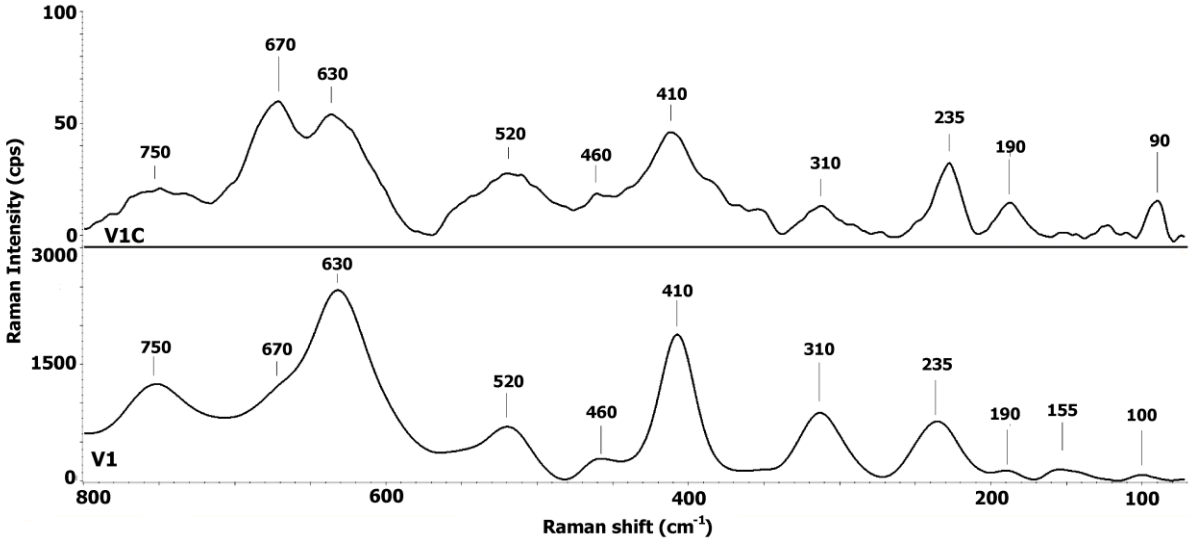

Fig. 5: Raman spectra of natural and acid treated vermiculites (V1 and V1C)

DSpace VŠB-TUO http://hdl.handle.net/10084/101847 26/5/2014

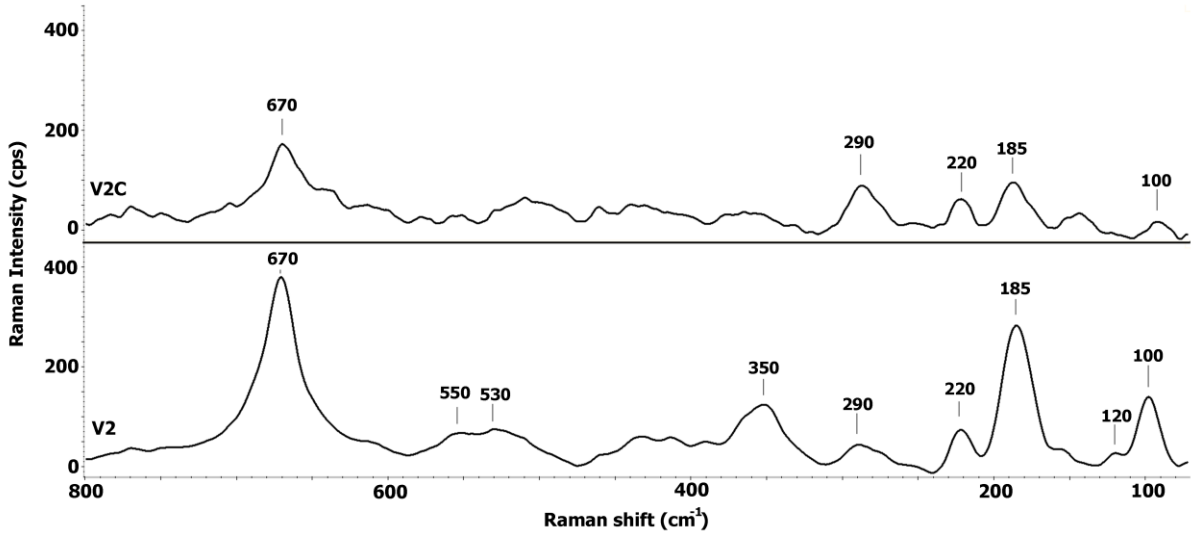

Fig. 6: Raman spectra of natural and acid treated vermiculites (V2 and V2C)

DSpace VŠB-TUO http://hdl.handle.net/10084/101847 26/5/2014